



# Well-confined Yb:GdVO<sub>4</sub> laser waveguide formed by MeV C<sup>3+</sup> ion implantation

Liang-Ling Wang<sup>a,\*</sup>, Jie Cheng<sup>a</sup>, Xiao-Jun Cui<sup>b</sup>

<sup>a</sup> Department of Physics and Information Engineering, Jining University, Xingtian Road, Qufu 273155, Shandong, China

<sup>b</sup> School of Science, University of Jinan, Jinan 250022, Shandong, China

## ARTICLE INFO

### Article history:

Received 30 August 2010

Received in revised form

13 December 2010

Accepted 13 December 2010

Available online 21 December 2010

### PACS:

61.80.-x

42.70.Hj

42.65.Wi

### Keywords:

Ion irradiation effects

Laser materials

Nonlinear waveguide

## ABSTRACT

The planar waveguide in *x*-cut Yb:GdVO<sub>4</sub> crystal has been fabricated by 6.0 MeV carbon ion implantation with the fluence of  $1 \times 10^{14}$  ions/cm<sup>2</sup> at room temperature. The modes of the waveguide were measured by the prism-coupling method with the wavelength of 633 nm and 1539 nm, respectively. An enhanced ordinary refractive index region was formed with a width of about 4.0 μm beneath the sample surface to act as a waveguide structure. By performing a modal analysis on the observed transverse magnetic polarized modes, it was found that all the transverse magnetic polarized modes can be well-confined inside the waveguide. Strong Yb-related photoluminescence in Yb:GdVO<sub>4</sub> waveguide has been observed at room temperature, which reveals that it exhibits possible applications for integrated active photonic devices.

© 2010 Elsevier B.V. All rights reserved.

## 1. Introduction

Among solid-state laser host materials, rare-earth-doped vanadate waveguides have strong potential for integrated optoelectronics application. GdVO<sub>4</sub> is a promising vanadate laser crystal doped by Nd [1,2], Yb, and Tm in many applications. Yb-doped media generally have long radiative lifetimes (there is no concentration quenching effect for high Yb doping concentration) and high quantum efficiency. The doping Yb<sup>3+</sup> ions possess no up-conversion effect or excited state absorption, which greatly reduces thermal effects in the crystal.

The remarkable properties of the Yb:GdVO<sub>4</sub> crystal drew huge attentions for developing laser waveguide devices on it. Optical waveguide formation in crystals has been studied extensively for use in many applications, such as efficient and compact lasers, switches, couplers, and other integrated photonic devices. Recent research reveals that ion implantation may be a universal method for fabricating waveguide structures in most optical materials because it has four advantages: (1) superior controllability and reproducibility to other techniques, such as diffusion, ion exchange, and epitaxial growth [3,4]; (2) it offers the possibility to bury a waveguide at various depths below the substrate surface by chang-

ing the ion species and energies of the implantation [5]; (3) it may be the only effective way to fabricate permanent waveguides in some oxide crystals with low Curie temperatures, such as KNbO<sub>3</sub> [6] or SBN [7]; (4) it is a non-equilibrium physical method, the number of injected ions is very small, and many are located in the vast range of the end of the injection in the waveguide layer, there is almost no doping effect, be able to maintain the original crystalline components. In addition, through an appropriate thermal annealing, the color centers and point defects in the waveguide layer can be eliminated. So ion implantation waveguide can keep the original optical properties, is a very good "crystal waveguide" [8].

Compared with the light ion implantation that was mostly carried out in the earlier works, implantation of medium-mass ions, such as C, O, or Si, receives gradually more attentions for waveguide construction, since in these cases much lower fluence are needed, in such a way that manufacturing costs are reduced [9,10]. In the waveguides formed by medium-mass ion implantation, positive change of the refractive index occurred in the waveguide region. Then a waveguide was formed by a region of high refractive index bounded by regions of lower index (air and substrate) [11–13]. Since carbon-ion-implanted Nd:YVO<sub>4</sub> waveguides exhibit good fluorescence spectra, which could be further used for efficient laser emissions [14]. In this paper, we reported on, to our knowledge the first time, the study of the Yb:GdVO<sub>4</sub> enhanced refractive index well-confined planar waveguide formed by low fluence carbon ion implantation.

\* Corresponding author. Tel.: +86 537 3196106; fax: +86 537 4670000.  
E-mail address: [wlling.jnxy@126.com](mailto:wlling.jnxy@126.com) (L.-L. Wang).

**Table 1**

The refractive indices of Yb:GdVO<sub>4</sub> crystal measured at both the wavelengths 633 nm and 1539 nm.

Wavelength (nm)	$n_e$	$n_o$
633	2.2434	2.0084
1539	2.1716	1.9592

## 2. Experimental details

The  $x$ -cut Yb:GdVO<sub>4</sub> crystal doped with 2 at% ytterbium was grown in the State Key Laboratory of Crystal Materials at Shandong University. The sample with size of 7 mm × 7 mm × 1.5 mm was optically polished and cleaned before ion implantation. The 7 mm × 7 mm face was implanted with 6.0 MeV C ions with the fluence of  $1 \times 10^{14}$  ions/cm<sup>2</sup>. In order to minimize the channeling effect during the implantation, the sample was tilted by 7° off the incident beam direction. The ion beam was electrically scanned to ensure a uniform implantation. The ion implantation was performed at room temperature by a 1.7 MV tandem accelerator at Peking University.

The dark modes of the Yb:GdVO<sub>4</sub> waveguide were measured by the standard prism-coupling technique (Metricon, USA) with an accuracy of 0.0002. A laser beam at wavelength of 633 nm (He–Ne laser) and 1539 nm (diode laser) stroke at the base of a prism, and hence the laser beam is coupled into waveguide region. A photodetector is used to detect the reflected beam. The prism, waveguide and photodetector were mounted on a rotary table. The intensity of the reflected light is plotted as a function of incident angle, where a sharp dip in the intensity profile would correspond to a possible mode. The refractive indices of the virgin Yb:GdVO<sub>4</sub> crystal were measured at both the wavelengths 633 nm and 1539 nm, see Table 1.

Photoluminescence (PL) spectroscopy in the region of the intra-4f transition from <sup>2</sup>F<sub>5/2</sub> to <sup>2</sup>F<sub>7/2</sub> of Yb<sup>3+</sup> ions was performed using the 976 nm line of a semiconductor laser as excitation source at room temperature. A Yokogawa AQ-6315A optical spectrum analyzer (OSA) with a resolution of 2 nm was used to measure PL spectroscopy.

## 3. Results and discussion

### 3.1. Numerical simulation of the implantation process

For the ion-implanted waveguides in photoelectrical materials, a major effect of ion implantation is the modification of the refractive index. The change of the refractive index depends on the end-of-ion range damage barriers due to nuclear collision cascades, leading to the partial lattice disorder accompanying a physical density reduction and a reduction of refractive index. When the implant distribution is Gaussian, the depth profile can be described by a projected range  $R_p$  and a range straggling  $\Delta R_p$ , which is the standard deviation of the Gaussian distribution in depth. We used the SRIM'2006 (The Stopping and Range of Ions in Matter) code to simulate the process of ion implantation with 6.0 MeV C ions into Yb:GdVO<sub>4</sub> crystal [15]. From Fig. 1 one can clearly see that most of the energy of the ion is lost in the electronic processed. The total number of target vacancies created by nuclear collisions is distributed in a peak near the end of ion track. The center of the distribution is at about 4.0 μm. Very few nuclear collision events happen in the region where the ion is traveling fast, which is dominated by ionization. The ion range is also distributed in a peak, the center of which is at about 4.2 μm, that is, slightly deeper than the damage distribution center. The mean projected ranges  $R_p$  and range straggling  $\Delta R_p$  values of C ions in Yb:GdVO<sub>4</sub> were calculated by SRIM'2006 code to be 4.0534 and 0.2817 μm, respectively.

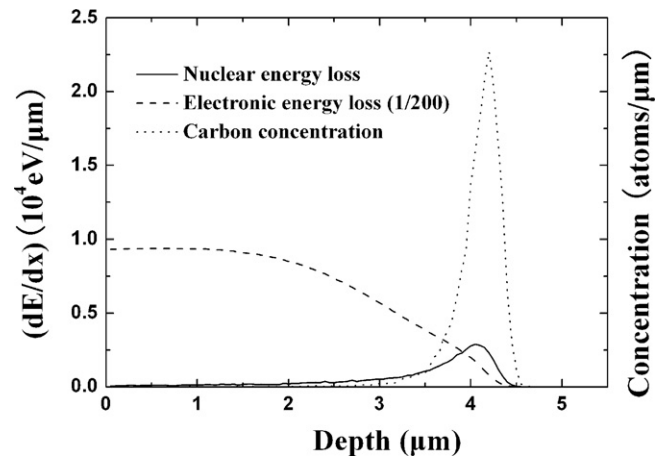


**Fig. 1.** The normalized electronic energy loss, nuclear energy loss and ion range distribution versus penetration depth of the 6.0 MeV C<sup>3+</sup> implanted into Yb:GdVO<sub>4</sub> crystal based on SRIM'2006.

### 3.2. Measurement of the waveguide by prism-coupling method

Fig. 2 shows measured relative intensity of polarized light as a function of the effective refractive index  $n_o$  (transverse magnetic (TM) polarized) and  $n_e$  (transverse electric (TE) polarized) for the planar Yb:GdVO<sub>4</sub> waveguide formed by 6.0 MeV C<sup>3+</sup> ions with a fluence of  $1 \times 10^{14}$  ions/cm<sup>2</sup> at the wavelength of 633 nm. When the light was coupled into the waveguide, a lack of reflected light would result in a dip in intensity. The refractive indices of the virgin Yb:GdVO<sub>4</sub> crystal were marked for comparison. When 633 nm laser beam was employed, clearly four TM modes (Fig. 2(a)) with higher index than bulk are observed. For the TE modes (Fig. 2(b)), only one mode was observed at 632.8 nm while no mode at 1539 nm. The effective refractive index of the mode ( $n_{eff} = 2.1413$ ) in Fig. 2(b) is lower than the refractive index of the substrate ( $n_{sub} = 2.2434$ ). When a 1539 nm laser beam was employed, as indicated in Fig. 3, two TM modes were observed, and their effective refractive indices ( $n_{eff} = 2.0265$  and  $1.9815$ ) were higher than those of the substrate ( $n_{sub} = 1.9592$ ). The refractive indices of uniaxial crystal satisfy  $n_x = n_y = n_o$ ,  $n_z = n_e$ ,  $n_o$  is the ordinary light refractive index,  $n_e$  is the extraordinary light refractive index. According to the relative size of the  $n_o$  and  $n_e$ , uniaxial crystal can be divided into two categories:  $n_e > n_o$ , known as the positive uniaxial crystal;  $n_e < n_o$ , known as the negative uniaxial crystal [16]. LiNbO<sub>3</sub> crystal is negative uniaxial crystal,  $n_e < n_o$ , when MeV low-fluence heavy-ion implantation occurs into LiNbO<sub>3</sub> crystal, the extraordinary refractive index increases. Yb:GdVO<sub>4</sub> crystal is positive uniaxial crystal,  $n_e > n_o$ , when Yb:GdVO<sub>4</sub> crystal was implanted by MeV low-fluence heavy-ions, an unusual type optical waveguide can be fabricated with ordinary refractive index increase. For the ion implanted Yb:GdVO<sub>4</sub> crystal ordinary light refractive index increases, while an exception to reduce the phenomenon of optical refractive index may be due Yb:GdVO<sub>4</sub> ( $\Delta n \approx 0.235$ ), ion implantation caused crystal with high birefringence phenomena (by waveguide region). Damage was mainly a number of isolated point defects and ion-for-bit, at low fluence, these injuries are often caused by disturbance and distortion of the lattice; for the phenomenon of high birefringence crystal will cause the higher refractive index lowered and the lower refractive index elevated [17].

### 3.3. Refractive index reconstruction

According to the dark-mode spectroscopy (Fig. 2(a)), we reconstruct the refractive index profile of the waveguide through reflectivity calculation method (RCM) [18], which has been proved

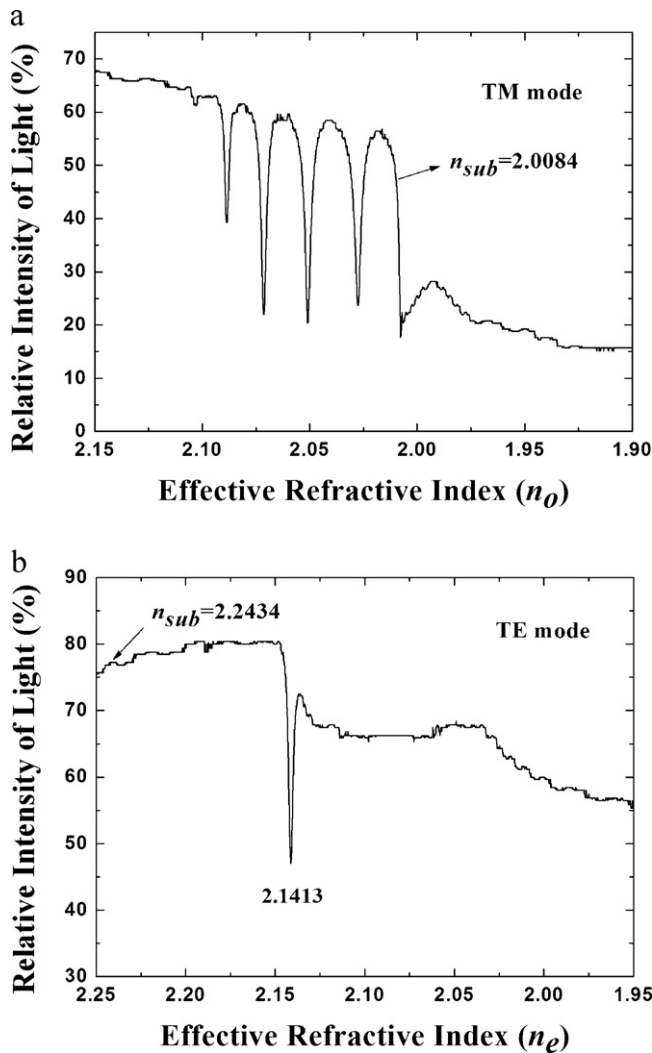


Fig. 2. Measured relative intensity of TM and TE polarized light reflected from the prism versus the effective refractive indices of the incident light for the planar Yb:GdVO<sub>4</sub> waveguide formed by 6.0 MeV C<sup>3+</sup> ions at fluence of 1 × 10<sup>14</sup> ions/cm<sup>2</sup> at the wavelength of 633 nm.

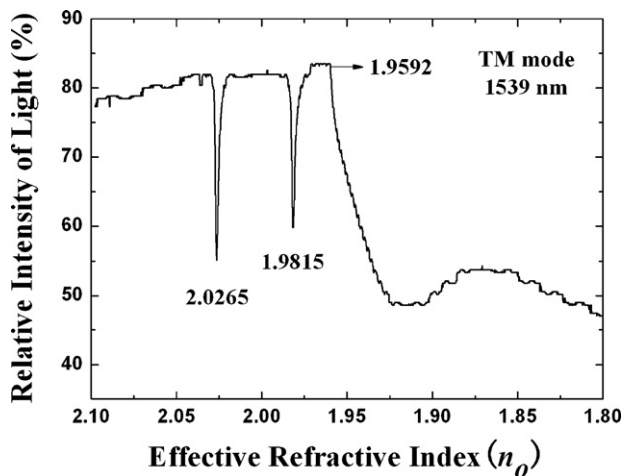


Fig. 3. Measured relative intensity of TM polarized light reflected from the prism versus the effective refractive indices of the incident light for the planar Yb:GdVO<sub>4</sub> waveguide formed by 6.0 MeV C<sup>3+</sup> ions at fluence of 1 × 10<sup>14</sup> ions/cm<sup>2</sup> at the wavelength of 1539 nm.

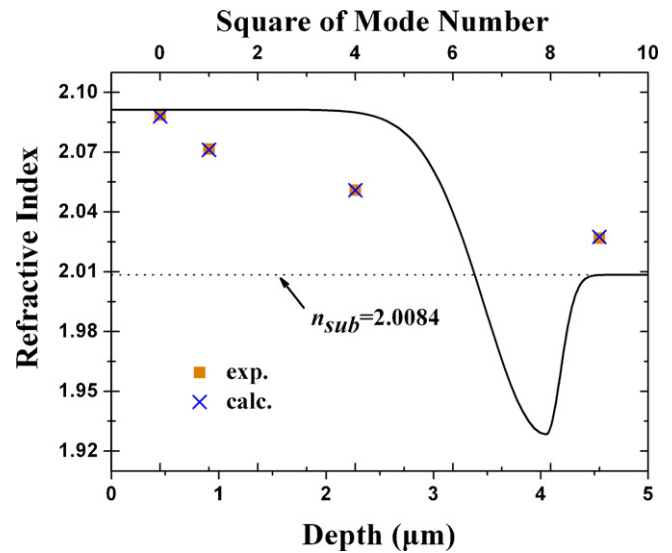


Fig. 4. Reconstructed refractive index  $n_o$  of the Yb:GdVO<sub>4</sub> waveguide formed by 6.0 MeV C<sup>3+</sup> ion implantation. Filled squares, experimental index values; crosses, calculated values based on the RCM.

to be particularly successful for ion implanted waveguides. In the present work, a least-squared fitting program based on RCM is available to calculate the refractive index profile by adjusting certain parameters until the theoretical mode indices match the experimental ones within a satisfactory error. Fig. 4 depicts the refractive index profile of the Yb:GdVO<sub>4</sub> waveguide formed by 6.0 MeV C ion implantation with the fluence of 1 × 10<sup>14</sup> ions/cm<sup>2</sup> reconstructed by the RCM at 633 nm. The refractive index ( $n_o$ ) of the virgin Yb:GdVO<sub>4</sub> crystal is also presented (dotted line) for comparison. As indicated in Fig. 4, the refractive index profile has one barrier, where the refractive index has a maximum decrease compared with the substrate. An enhanced ordinary refractive index region was formed with a width of about 4.0 μm beneath the sample surface to act as a waveguide structure. As it is shown, compared to the refractive index profile (Fig. 4) with the energy loss (Fig. 1), the near-surface damage correlated to electronic stopping, which causes an increase of the ordinary refractive index, and end-of-ion range damage generated by collision cascades, which decreases the ordinary refractive index values [19]. Nevertheless, a detailed understanding needs further investigation.

Table 2 shows the comparison of the measured mode indices with the calculated value of the indices by RCM propagation in the Yb:GdVO<sub>4</sub> waveguide obtained at the wavelength of 633 nm. It is found that the measured effective refractive indices were in agreement with the calculated values with less than 10<sup>-4</sup>.

### 3.4. Modal analysis

By using a beam propagation method (BPM) [20], we investigated the confinement of the light in the waveguide when possible modes are excited. Fig. 5 shows the field intensity distribution of TM (magnetic field strength versus depth) modes for the Yb:GdVO<sub>4</sub>

Table 2  
Comparison of measured and calculated values by RCM propagation modes of their effective refractive indices obtained at the wavelength of 633 nm.

Mode number	Measured	Calculated	Difference
1	2.0886	2.0880	0.0006
2	2.0716	2.0712	0.0004
3	2.0509	2.0509	0.0000
4	2.0268	2.0275	-0.0007

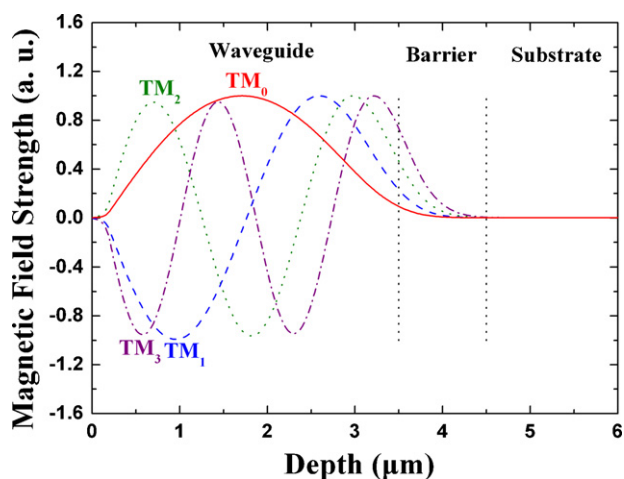


Fig. 5. Field intensity distribution of  $TM_0$  (solid),  $TM_1$  (dash),  $TM_2$  (dot) and  $TM_3$  (dash dot) modes for the Yb:GdVO<sub>4</sub> waveguide formed by 6.0 MeV C<sup>3+</sup> ion implantation at the fluence of  $1 \times 10^{14}$  ions/cm<sup>2</sup>.

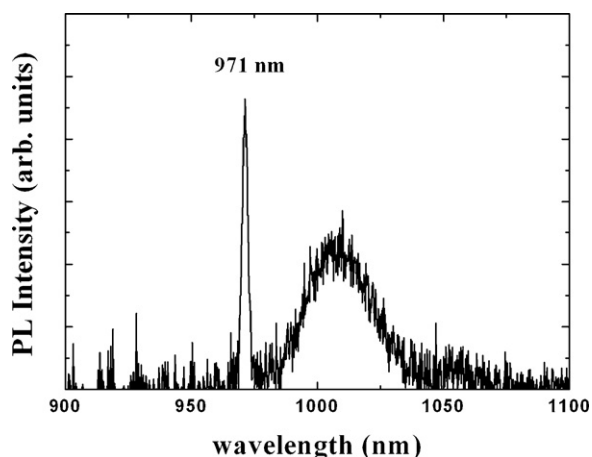


Fig. 6. PL spectrum of Yb:GdVO<sub>4</sub> waveguide measured at room temperature. The pump wavelength is 976 nm.

waveguide formed by C<sup>3+</sup> ion implantation at the fluence of  $1 \times 10^{14}$  ions/cm<sup>2</sup>. The feature to be noted here is that all the field profiles in the substrate region are not oscillating but evanescent. As a result, the tunneling effect can be inhibited in this waveguide structure. It is found from Fig. 6 that  $TM_0$  mode has the smallest depth of penetration, which means that this mode can be completely confined in the waveguide region. As it is indicated, the field of  $TM_1$ ,  $TM_2$  and  $TM_3$  is almost restricted within the guide region, which makes these to be the guiding modes.

### 3.5. Photoluminescence measurement

The intra-4f-shell luminescence of rare-earth (RE) ions in crystals is well-known to show sharp and intense peaks even at room temperature. For the purpose of practical applications involving optical gain, it is necessary to investigate the photoluminescence properties of the active waveguide. However, thermal quenching phenomenon appears to strongly suppress the intra-4f-transition PL when the temperature is higher than 100 K [21]. Fig. 6 shows the room temperature PL spectra corresponding to the  ${}^2F_{5/2} \rightarrow {}^2F_{7/2}$  laser transition of Yb<sup>3+</sup> ions from the Yb:GdVO<sub>4</sub> planar waveguide. Such sharp PL peaks suggest that Yb ion forms only one kind of

the emission center at 970 nm, which was caused by the transition  ${}^2F_{5/2} \rightarrow {}^2F_{7/2}$  of Yb<sup>3+</sup> ions. Besides it, a remarkable broad PL band peak located at about 1010 nm was found in an Yb:GdVO<sub>4</sub> spectrum. The PL band should be related to the Yb ion state and may play an important role for the excitation process [22].

## 4. Summary

In summary, we have demonstrated the fabrication and characterization of planar waveguide in *x*-cut Yb:GdVO<sub>4</sub> crystal by 6.0 MeV C<sup>3+</sup> ion implantation with a fluence of  $1 \times 10^{14}$  ions/cm<sup>2</sup>. The dark mode spectra were measured by the prism coupling method. The reconstructed refractive index profile includes a non-leaky guiding region which can confine the light efficiently. The beam propagation method is used to calculate the magnetic field profiles in the waveguide region from the reconstructed refractive index profile, which indicates that the refractive index increased waveguide layer can confine the mode almost completely. The efficient Yb<sup>3+</sup>-related emission in Yb:GdVO<sub>4</sub> was observed at room temperature, which implies attractive potentials for highly efficient integrated lasers based on the Yb:GdVO<sub>4</sub> waveguide.

## Acknowledgments

Authors would like to thank Zhao-Jun Liu for his help in the PL spectra measurement. This work is supported by the Promotive Research Fund for Excellent Young and Middle-aged Scientists of Shandong Province, China (Grant No BS2010CL008), Project of Shandong Province Higher Educational Science and Technology Program (Grant No J10LA56), and Jining University of Youth Research Fund (Grant No 2009QNKJ01).

## References

- [1] S.V. Garnov, S.A. Solokhin, E.D. Obratsova, A.S. Lobach, P.A. Obratsov, A.I. Chernov, V.V. Bukin, A.A. Sirotkin, Y.D. Zagumennyi, Y.D. Zavartsev, S.A. Kutovoi, I.A. Shcherbakov, *Laser Phys. Lett.* 4 (2007) 648.
- [2] T.T. Basiev, S.V. Vassiliev, V.A. Konjushkin, V.V. Osiko, A.I. Zagumennyi, Y.D. Zavartsev, S.A. Kutovoi, I.A. Shcherbakov, *Laser Phys. Lett.* 1 (2004) 237.
- [3] P.D. Townsend, P.J. Chandler, L. Zhang, *Optical Effects of Ion Implantation*, Cambridge University Press, Cambridge, 1994.
- [4] S. Takahashi, P. Dawson, A.V. Zayats, L. Bischoff, O. Angelov, D. Dimova-Malinovska, T. Tsvetkova, P.D. Townsend, *J. Phys. D* 40 (2007) 7492.
- [5] F. Schrepel, T. Opfermann, J.-P. Ruske, U. Grusemann, W. Wesch, *Nucl. Instrum. Methods B* 218 (2004) 209.
- [6] D. Fluck, T. Pliska, P. Günter, St. Bauer, L. Beckers, Ch. Buchal, *Appl. Phys. Lett.* 69 (1996) 4133.
- [7] D. Kip, S. Aulkemeyer, P. Moretti, *Opt. Lett.* 20 (1995) 1256.
- [8] H. Hu, F. Lu, F. Chen, F.X. Wang, J.H. Zhang, X.D. Liu, K.M. Wang, B.R. Shi, *Opt. Commun.* 177 (2000) 189.
- [9] L.L. Wang, L. Wang, K.M. Wang, Q.M. Lu, H.J. Ma, *Opt. Express* 17 (2009) 5069.
- [10] F. Chen, Y. Tan, L. Wang, Q.M. Lu, H.J. Ma, *J. Phys. D* 40 (2007) 5824.
- [11] D. Jaque, F. Chen, Y. Tan, *Appl. Phys. Lett.* 92 (2008) 161908.
- [12] G.G. Bentini, M. Bianconi, M. Chiarini, L. Corraera, C. Sada, P. Mazzoldi, N. Argiolas, M. Bazzan, R. Guzzi, *J. Appl. Phys.* 92 (2002) 6477.
- [13] G.V. Vázquez, J. Rickards, G. Lifante, M. Domenech, E. Cantelar, *Opt. Express* 11 (2003) 1291.
- [14] G.V. Vázquez, M.E. Sanchez-Morales, H. Marquez, J. Rickards, R. Trejo-Luna, *Opt. Commun.* 240 (2004) 351.
- [15] J.F. Ziegler, J.P. Biesack, U. Littmark, *The Stopping and Range of Ions in Matter*, Pergamon, New York, 1985.
- [16] C.Y. Gao, H.R. Xia, J.Q. Xu, S.C. Si, H.J. Zhang, J.Y. Wang, *Cryst. Res. Technol.* 43 (2008) 443.
- [17] J. Rams, J. Olivares, P.J. Chandler, P.D. Townsend, *J. Appl. Phys.* 87 (2000) 3199.
- [18] P.J. Chandler, F.L. Lama, *Opt. Acta* 33 (1986) 127.
- [19] G.G. Bentini, M. Bianconi, L. Corraera, M. Chiarini, P. Mazzoldi, C. Sada, N. Argiolas, M. Bazzan, R. Guzzi, *J. Appl. Phys.* 96 (2004) 242.
- [20] D. Yevick, W. Bardyszewski, *Opt. Lett.* 17 (1992) 329.
- [21] A. Taguchi, H. Nakagome, K. Takahai, *J. Appl. Phys.* 70 (1991) 5604.
- [22] K. Sato, T. Takamasu, G. Kido, *J. Appl. Phys.* 95 (2004) 2924.